# Performance Analysis of PMSG Based Wind Energy Conversion System

Manpreet Kaur, Prince Jindal
*BGIET, Sangrur, Punjab, India*

***Abstract*** **-** This paper PMSG based wind power conversion system with constant wind speed,variable wind speed and different fault condition is investigated.The WECS is based on PMSG fed by AC/DC/AC converte.The proposed controller provided a variable voltage variable frequency source into a fixed voltage fixed frequency supply. Generic three-phase AC-DC-AC converter, converter control methods for wind power generation, wind turbine, two mass drive train and PMSG generator are modeled in the thesis using MATLAB / SIMULINK for establishing variable-speed wind energy conversion systems. The developed wind energy conversion system have been validated through simulation study using MATLAB / SIMULINK, under different input/output conditions like constant wind speed, variable wind speed, and different fault conditions. The simulation results verify the validity of the developed wind energy conversion system and its controls.

***Keywords:*** *AC-DC-AC converter, PMSG, two mass drive train, wind turbine,wind energy*

## I. INTRODUCTION

In recent years, there has been an increasing awareness about the global warming and the harmful effects that the emissions of carbon have. This created a higher demand for clean and sustainable energy sources like: wind, sea, sun, biomass etc. The wind energy has experienced the biggest growth in the past 10 years. This is because wind energy is a pollution-free resource, has an inexhaustible potential and also because of its increasingly competitive cost. The size of the wind turbine installations has also grown from 300 KW in the early 1990, up to 10 MW capacity range presently. The main drawback of the wind is that it is irregular in occurrence. The problem becomes how to maximize the energy capture from the wind. The wind energy can be harnessed by a wind energy conversion system (WECS), composed of a wind turbine, an electric generator, a power electronic converter and the corresponding control system. Based on the types of components used, different WECS structures can be realized. However, the objective in all structures is the same, i.e., the wind energy at varying wind velocities has to be converted to electric the grid frequency.

In terms of generators for wind power-application, there are two main classes considering the speed: constant and variable speed. The constant speed wind turbines and induction generators were often used, in the early stages of wind power development. Some of the disadvantages of the fixed speed generators are the low efficiency, poor power quality, high mechanical stress but also that by having a fixed speed operation the maximum coefficient of performance is obtained only at a particular wind speed. Due to development of power electronics and their falling costs, the variable speed operation became the most attractive option. By running the wind turbine generator in variable speed, variable frequency mode, and the maximum power can be extracted, at low and medium wind speeds. Among all kinds of wind energy conversion systems (WECSs), a variable speed wind turbine (WT) equipped with a multi pole permanent magnet synchronous generator (PMSG) is found to be very attractive and suitable for application in large wind farms. With gearless construction, such PMSG concept requires low maintenance, reduced losses and costs, high efficiency and good controllability. Currently, the PMSG-based WECS has been commercialized by some WT manufactures, such as Siemens Power Generation and GE Energy.

### *A. Conventional constact speed wind energy system*

In conventional fixed speed type the wind turbine is directly or with gear is connected to grid as shown in Figure 1.

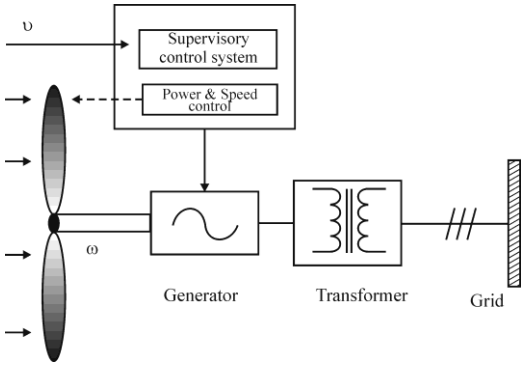


Fig. 1: Fixed speed type wind energy conversion system

### *B. Variable speed wind generating system*

A variable speed wind generating system connected to the grid is shown in Figure 2.

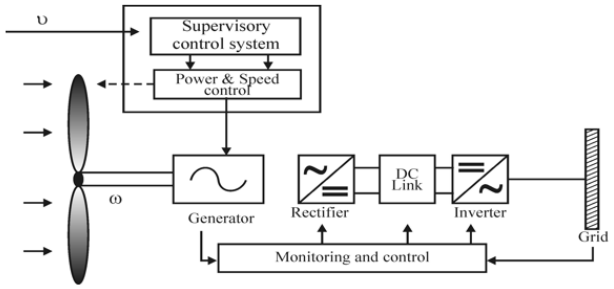


Fig. 2: Variable speed type wind energy conversion

### *C. Wind turbine configuration*

The generator is connected through a full scale voltage source converter: generator converter is used to control the torque and the speed and grid side converter used to control the power flow in order to keep the DC-link voltage constant.

The two converters are connected by a DC link capacitor in order to have a separate control for each converter. In Figure 3 the PMSG and the full scale converter are presented.

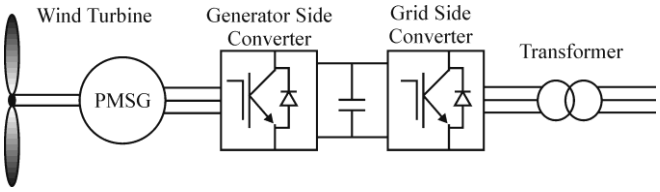


Fig. 3: Wind turbine configuration

## II. MODELLING OF THE WIND ENERGY CONVERSION SYSTEM

In this paper, various design and modelling aspects of different components of the WECS System like the basic models of synchronous generator, AC-DC-AC PWM converter, wind turbine, drive train and their control system are discussed in detail.

### *A. The Proposed Wind Energy Conversion System*

As it can be seen in Fig.1, the proposed WECS system consists of wind turbine, two mass drive train, permanent magnet synchronous machine (PMSM) which is torque controlled and AC-DC-AC PWM converter.

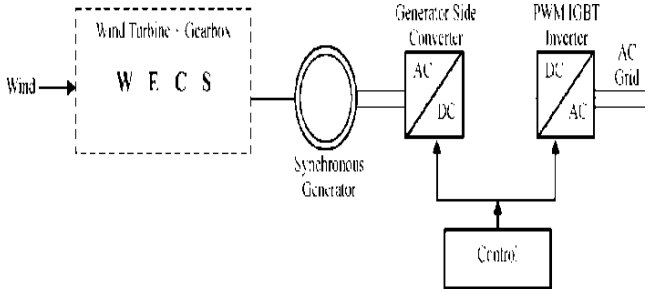


Fig. 4: Proposed Wind Energy Conversion System

### *B. Permanent Magnet Synchronous Generator (PMSG)*

The PMSG is a Synchronous Machine, where the DC excitation circuit is replaced by permanent magnets, by eliminating the brushes. PMSG has a smaller physical size, a low moment of inertia which means a higher reliability and power density per volume ratio as it has permanent magnets instead of brushes and the slip rings. Also by having permanent magnets in the rotor circuit, the electrical losses in the rotor are eliminated. Because of above mentioned advantages, the PMSG are becoming an interesting solution for wind turbine applications.

### *C. Three Phase PMSG d-q Model*

The voltage of a 3-phase PMSG in the phase coordinate frame can be expressed as

$$(1)\begin{cases} u_A = U_m \sin \omega t \\ u_B = U_m \sin\left(\omega t - \frac{2\pi}{3}\right) \\ u_C = U_m \sin\left(\omega t + \frac{2\pi}{3}\right) \end{cases}$$

where Um is the magnitude of the phase voltage and w is the angular frequency of the voltage in the phase coordinate frame. (1) can be transformed to the d-q axis through the following transformation matrix

$$\begin{bmatrix} u_d \\ u_q \\ u_0 \end{bmatrix} = \sqrt{\frac{2}{3}} \begin{bmatrix} \cos\theta_r & \cos\left(\theta_r - \frac{2\pi}{3}\right) & \cos\left(\theta_r + \frac{2\pi}{3}\right) \\ -\sin\theta_r & -\sin\left(\theta_r - \frac{2\pi}{3}\right) & -\sin\left(\theta_r + \frac{2\pi}{3}\right) \\ \sqrt{\frac{1}{2}} & \sqrt{\frac{1}{2}} & \sqrt{\frac{1}{2}} \end{bmatrix} \begin{bmatrix} u_A \\ u_B \\ u_C \end{bmatrix} \quad (2)$$

Where $\theta_r$ is the rotor position, $\theta_r = \theta_0 + f\omega dt$, $\theta_0$ is the initial position of the rotor.

After the transformation, the performance of a PMSG can be described by the parameters given in the next few paragraphs.

The PMSG voltage is described by

$$\begin{bmatrix} u_d = \frac{d\psi_d}{dt} - \omega\psi_q - R_d i_d \\ u_q = \frac{d\psi_q}{dt} - \omega\psi_d - R_q i_{dq} \end{bmatrix} \quad (3)$$

where Rd and Rq are the d- and q-axis resistance. For the PMSGs studied in this thesis, Rd = Rq = R1, where R1 is the phase resistance of the PMSG. $\psi_d$ and $\psi_q$ are the d- and q-axis fluxes, and id and iq are the d-and q-axis currents.

The PMSG flux is described by

$$\begin{cases} \psi_d = L_d i_d + L_{ad} i_{fm} \\ \psi_q = -L_q i_q \end{cases} \quad (4)$$

where Lad is the d-axis armature reaction inductance and L1 is the leakage inductance Ld and Lq are the d- and q-axis synchronous inductance,

$$L_d = L_{ad} + L_1$$
$$L_q = L_{aq} + L_1 \quad (5)$$

where Laq is the q-axis armature reaction inductance and ifm is the equivalent current of the magnet. The electromagnetic torque is described by

$$T_{em} = p(\psi_d i_q - \psi_q i_d$$
$$= p[L_{ad} i_{fm} i_q - (L_q - L_q) i_d i_q] \quad (6)$$

where p is the number of pole-pairs. The mechanical equation of PMSG is described by

$$J = \frac{d\Omega}{dt} = T_{mec} - T_{em} - R_\Omega \Omega \quad (7)$$

where J is the rotational moment of inertia, Ω is the mechanical angular speed, Tmec and Tem are the turbine mechanical drive torque and the PMSG electromagnetic torque, and $R_\Omega$ is the damping coefficient. The damping coefficient can be calculated from

$$R_\Omega = \begin{cases} \dfrac{P_{fw}}{\Omega^2} & \Omega \le \Omega_N \\ \dfrac{P_{fw}}{\Omega^2} & \Omega > \Omega_N \end{cases} \quad (8)$$

where $\Omega_N$ is the rated PMSG angular mechanical speed and pfw is the mechanical loss under rated load conditions.

*A. AC-DC-AC PWM Converters*

The equivalent circuit of a voltage source converter is presented in Fig.5.As it can be seen in the figure, a three phase converter has 6 semiconductors (IGBTs) displayed in three legs: a, b and c. The 6 semiconductors are considered as ideal switches. Only one switch on the same leg can be conducting at the same time.

In the figure, Sa, Sb, Sc are variables which represent the switching status for each leg. Scan only have two values: 1 for the conduction state and 0 for the block state.

The desired output voltages are obtained by programming the duty cycles of the 6 IGBTs

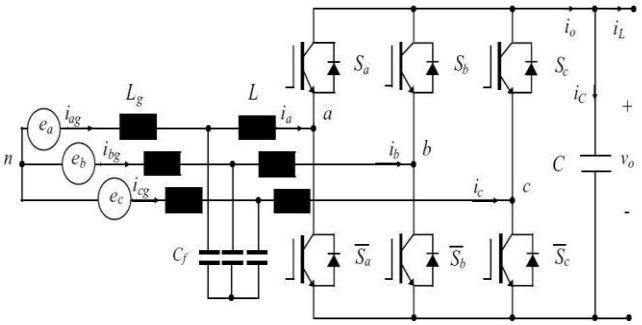


Fig. 5 :VSC with ideal switches

The phase voltages are calculated using the DC voltage and the duty cycles Da, Db, Dc

$$\left.\begin{aligned} u_{a0} &= \frac{U_{DC}}{3}(2D_a - D_b - D_c) \\ u_{a0} &= \frac{U_{DC}}{3}(-D_a - 2D_b - D_c) \\ u_{a0} &= \frac{U_{DC}}{3}(-D_a - D_b - 2D_c) \end{aligned}\right\} \quad (9)$$

where, ua0, ub0, uc0 - phase voltages; UDC - DC voltage.The DC link current can be expressed as:

$$i_{DC} = [D_a D_b^{'} D_c].\begin{bmatrix} i_a \\ i_b \\ i_c \end{bmatrix} \quad (10)$$

where ia, ib, ic - line currents.

*B. Wind Turbine and Pitch Controller*

The turbine is the prime mover of WECS that enables the conversion of kinetic energy of wind Ew into mechanical power Pm and eventually into electricity

$$\begin{cases} P_m = \dfrac{\partial E_w}{\partial t} C_p = \dfrac{1}{2}\rho A V_w^3 C_p \\ C_p(\lambda,\beta) = 0.5176\left(\dfrac{116}{\lambda_1} - 0.4\beta - 5\right)e^{-21/\lambda_1} + 0.0068\lambda \end{cases} \quad (11)$$

where Vw is the wind speed at the center of the rotor (m/sec), ρ is the air density (Kg/m3), A = ΠR² is the frontal area of the wind turbine (m2) and R is the rotor radius.

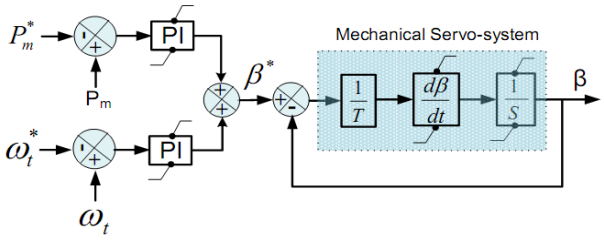


Fig. 6: Pitch angle control scheme using PI controllers

Cp is the performance coefficient which in turn depends upon the turbine characteristics (ß -blade pitch angle and λ-tip speed ratio) that is responsible for the losses in the energy conversion process.

The numerical approximation of Cp used in this study is taken from and $\lambda_i = f(\lambda, \beta)$ is given by

$$\begin{cases} P_m = \dfrac{\omega_t R}{V_w} \\ \dfrac{1}{\lambda_1} = \dfrac{1}{\lambda + 0.08\beta} - \dfrac{0.035}{\beta^3 + 1} \end{cases} \quad (12)$$

where ωis the turbine speed and R is the blade radius of the wind turbine.

*C. Modelling of Two Mass Drive Train*

By applying Newton's second law for rotation system or using energy principles on the rotor, the mathematical model will be:

$$Jr\dot{w}_t + B_r w_t = T_a - T_{ls} \quad (13)$$

where Jr = rotor moment of inertia(cancelled), wt = rotor angle speed, Br = rotor damping effect, Ta = applied torque on the rotor, Tls = low speed shaft torque.

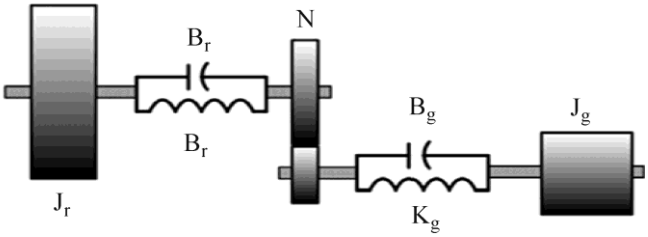


Fig.7: Two mass drive train model

Whereas the same technique is applied for the driving gear, which basically its moment of inertia is cancelled, this will yield:

$$J_{ls}\dot{w}_{ls} + B_{ls(w_t - w_{ls})} + K_{ls}(_t - _{ls}) = T_{ls} \quad (14)$$

Where J1s = drive moment of inertia, w1s = angular speed of the low speed shaft, B1s= low speed damping effect, K1s= stiffness of low speed shaft, qt= rotor angular displacement, q1s= low speed angular displacement.

This will yield

$$T_{ls} = B_{ls(w_t - w_{ls})} + K_{ls}(_t - _{ls}) \quad (15)$$

By the same procedure, the mathematical model for the generator is:

$$J_g\dot{w}_g + B_g w_g = T_{hs} - T_{em} \quad (16)$$

Where J1s = generator moment of inertia, wg = angular speed of high speed shaft, Bg= high speed damping effect, Tsh= high speed shaft torque, Tgen = generator electromagnetic torque,

The gear train ratio ng is described by

$$n_g = \frac{T_{ls}}{T_{hs}} = \frac{w_g}{w_{ls}} = \frac{g}{ls} \quad (17)$$

where, wg = is the angular displacement of high speed shaft.

## III IMPLEMENTATION OF WECS IN MATLAB / SIMULINK

Various components of the wind energy conversion system (WECS) like synchronous generator, AC-DC-AC PWM converter, wind turbine, drive train and their control system is implemented in MATLAB/SIMULINK environment.

### *A. Proposed AC-DC-AC PWM Converter based WECS Model*

In order to study the effects of the entire WECS, the proposed system is modelled using MATLAB/SIMULINK environment by using different toolboxes. It includes a wind turbine and drive train model, PMSG model, and AC-DC-AC PWM converter and its control model. The different block sets of SIMPOWER SYSTEM toolbox is specially used to design the electrical model. The proposed WECS system as shown is implemented using MATLAB/SIMULINK environment as shown in fig.8 proposed wind energy conversion system in MATLAB/SIMULINK is described in below sections.

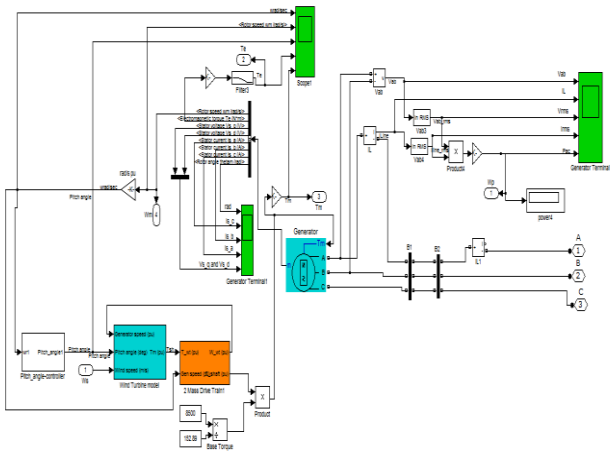

Fig.8: Proposed Wind Energy Conversion System in MATLAB/SIMULINK

### *B. Wind Turbine Model*

The wind turbine model designed in MATLAB/SIMULINK is shown in fig. 9. This block implements a variable pitch wind turbine model. The performance coefficient Cp of the turbine is the mechanical output power of the turbine divided by wind power and a function of wind speed, rotational speed, and pitch angle (beta). Cp reaches its maximum value at zero betas.

Various parameters of the wind turbine are designed as:

Nominal mechanical output power (W): 8.5e3

Base power of the electrical generator (VA): 8.5e3/0.9

Base wind speed (m/s): 8

Maximum power at base wind speed (p.u. of nominal mechanical power): 0.8

Base rotational speed (p.u. of base generator speed): 1

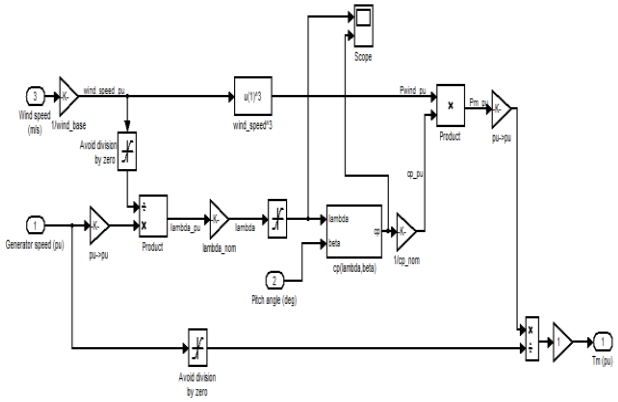


Fig.9 :Wind Turbine Model

### *C. Two Mass Drive Train Model*

The Two mass drive train model implemented in SIMULINK is shown in Fig.10.This is turbine and shaft

coupling system. The above subsystem will give shaft torque T_ shaft(pu),W_wtas outputs and T_wt(pu),generator speed(pu) as input .It is an example of closed loop control system where feedback is provided just before the gain (=1)

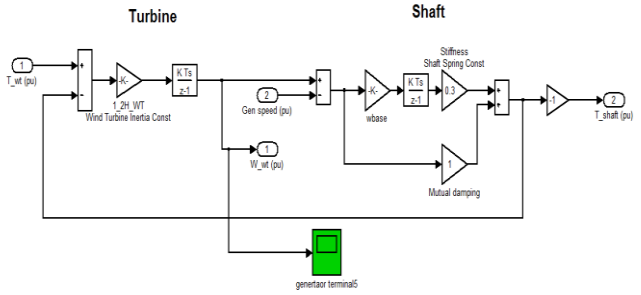


Fig.10: Two mass drive train model

*D.Pitch Angle Controller*

The Pitch angle controller designed in MATLAB/SIMULINK is shown in Fig.11. Here, pitch compensator is also designed with Proportional gain (Kp):1.5, Integral gain (Ki):6, output max. Limit: 45, min. limit: 0, Pitch Gain: 500.

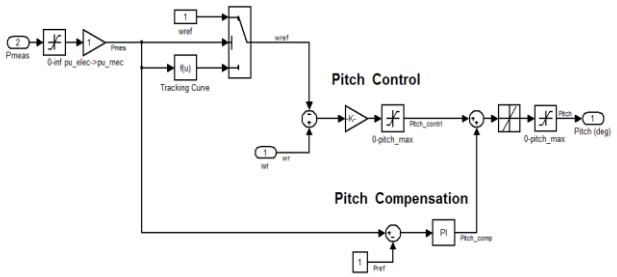


Fig.11: Pitch angle controller

*E. AC-DC-AC PWM Converters*

The PWM controller designed to produce the gate pulse is shown in fig.12. Voltage controller is also designed which is shown in fig. 13 with Proportional gain (Kp):0.4, Integral gain (Ki):500, Carrier frequency (Hz):2000. The abc_to_dqo Transformation, Discrete virtual PLL, Discrete PID Controller, dqo_to_abc Transformation, Discreate PWM generator developed in MATLAB/SIMULINK are shown in fig.12 to fig. 15. Fig 14 show the there is a error signal apply to proportional gain (Kp) and integral gain (Ki). proportional gain(Kp) apply to zero order hold The Zero-Order hold block samples and holds its input for the specified sample period The block accepts one input and generates one output, both of which can be scalar or vector If the input is a vector, all elements of the vector are held for the same sample period.

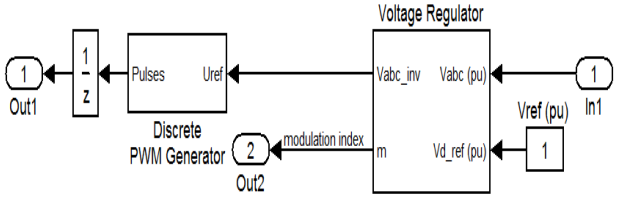


Fig. 12: PWM controller

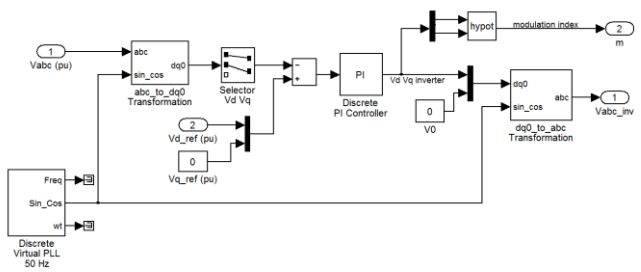


Fig .13: Voltage Controller

Integral gain (Ki) applies to Discrete-Time Integrator block in place of the Integrator block to create a purely discrete system. Both zero order hold and Discrete-Time Integrator block apply sum and saturation block and then got output. It is a closed loop control system that generates and outputs a signal in relation to the frequency and phase of an input (reference) signal. In the basic blocks a constant value is amplified then summed with an output of product block.

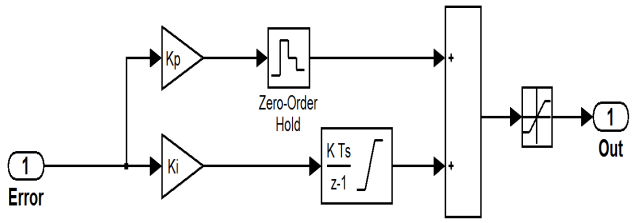


Fig.14 :Discrete PID Controller

It will give three outputs Freq, wt and sin_cos out which freq and wt is terminated. And only sin_cos will be propagated further. sin and cos are combined into one single input by mux.

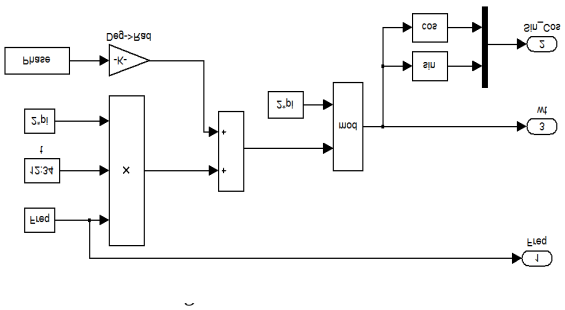

## IV SIMULATION RESULTS AND DISCUSSION

In this paper, simulation results of developed wind energy conversion system (WECS) connected to a utility grid under different conditions i.e. under constant wind speed, step change in wind speed, three phase to ground fault etc. are presented to validate the developed models and controls for the proposed wind generation system.

### Case-1 Under Fault Conditions At Grid Side

*A. Three Phase to Ground Fault (L-L-L-G)*

Here, to test the validity of the developed WECS system, three phase to ground fault has been applied at time t=0.4 sec. for a duration of 0.1 sec. after which, fault has been cleared.

Simulation results from fig. 28 to fig. 31 show the response of various parameters of the developed model during the fault condition. It can be seen that during the fault period, voltage becomes almost zero, current undergo transients, dc voltage becomes zero, grid voltage and current also becomes zero. After the fault period, parameters undergo transients and attain steady state within very short time, validating the developed model

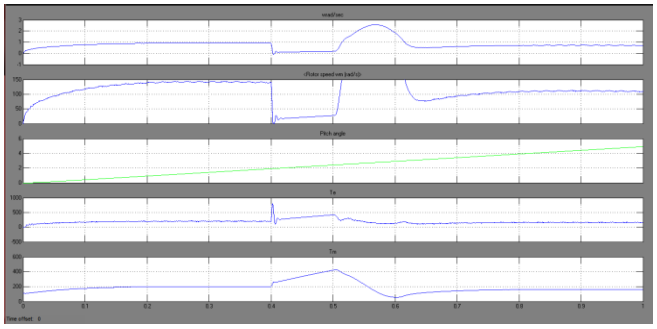

Fig. 15: Waveform of Synchronous generator Rotor wind speed Wm (rad/sec), Pitch Angle, Mechanical Torque (Tm), Electromagnetic Torque (Te)

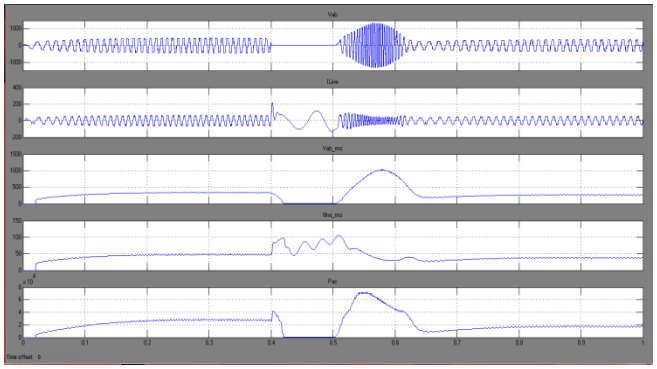

Fig. 16: Waveform of line to line Voltage (Vab), Line Current (IL), rms Line Voltage (Vab_rms), AC Power

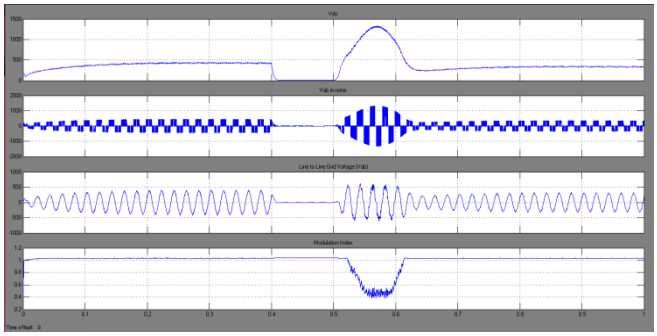

Fig. 17: Waveform of dc link voltage, Inverter output AC voltage, line to line grid voltage, and modulation Index

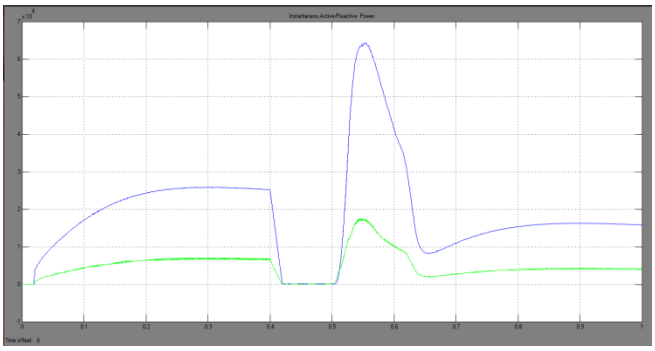

Fig. 18: Instantaneous Active and reactive power waveforms

*B. Two Phase to Ground Fault (L-L-G)*

Here, to test the validity of the developed WECS system, two phase to ground fault has been applied at time t=0.4 sec. for a duration of 0.1 sec. after which, fault has been cleared. Simulation results from fig. 32 to fig. 35 show the response of various parameters of the developed model during the fault condition. It can be seen that during the fault period, voltage becomes almost zero, current undergo transients, and dc voltage becomes zero, grid voltage and current also becomes zero. After the fault period, parameters undergo transients and attain steady state within very short time, validating the developed model

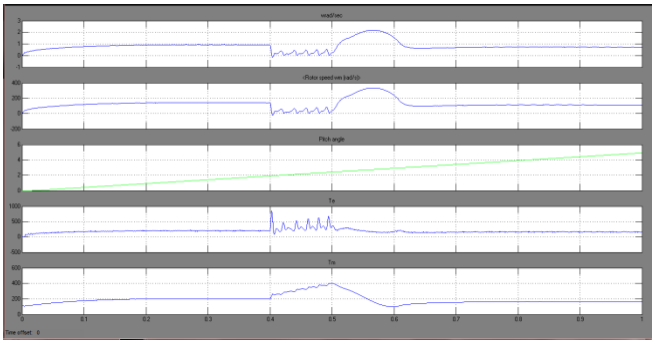

Fig. 19: Waveform of Synchronous generator Rotor wind speed Wm (rad/sec), Pitch Angle, Mechanical Torque (Tm), Electromagnetic Torque (Te)

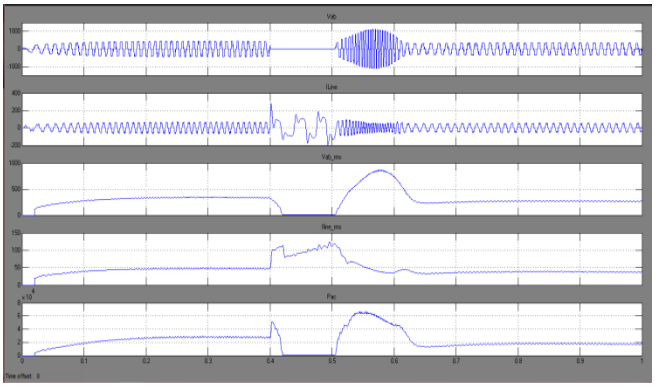

Fig. 20:Waveform of line to line Voltage (Vab), Line Current (IL), rms Line Voltage (Vab_rms), AC Power

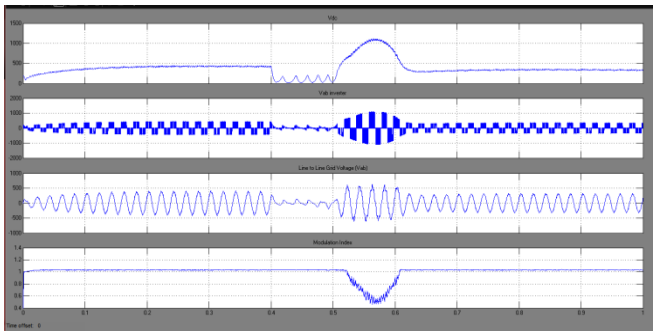

Fig. 21: Waveform of dc link voltage, Inverter output AC voltage, line to line grid voltage, and modulation Index.

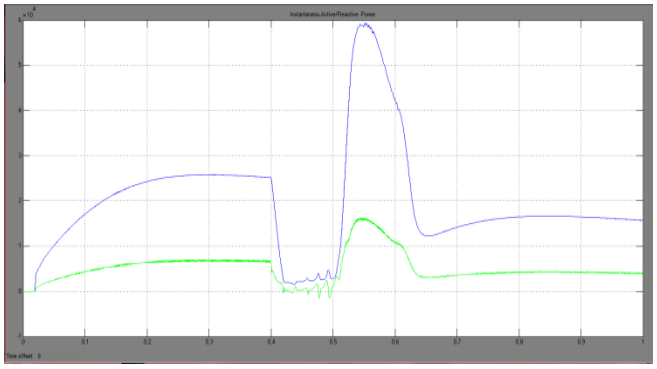

Fig. 22: Instantaneous Active and reactive power waveforms

### *C. Single Phase to Ground Fault (L-G)*

Here, to test the validity of the developed WECS system, single phase to ground fault has been applied at time t=0.4 sec. for duration of 0.1 sec. after which, fault has been cleared. Simulation results from fig.36 to fig. 40 show the response of various parameters of the developed model during the fault condition. It can be seen that during the fault period, voltage becomes almost zero, current undergo transients, and dc voltage becomes zero, grid voltage and current also becomes zero. After the fault period, parameters undergo transients and attain steady state within very short time, validating the developed model.

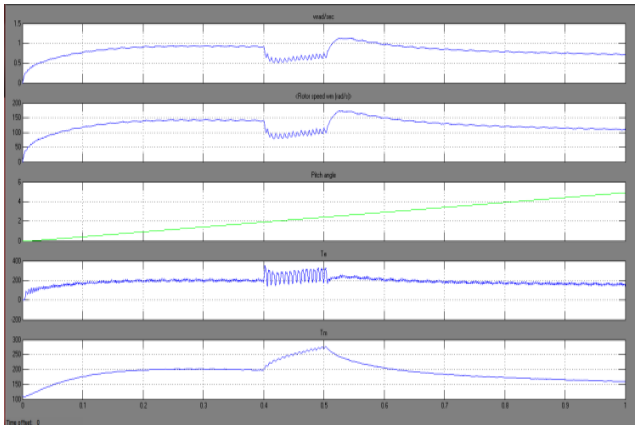

Fig. 23 Waveform of Synchronous generator Rotor wind speed Wm(rad/sec), Pitch Angle, Mechanical Torque (Tm), Electromagnetic Torque (Te)

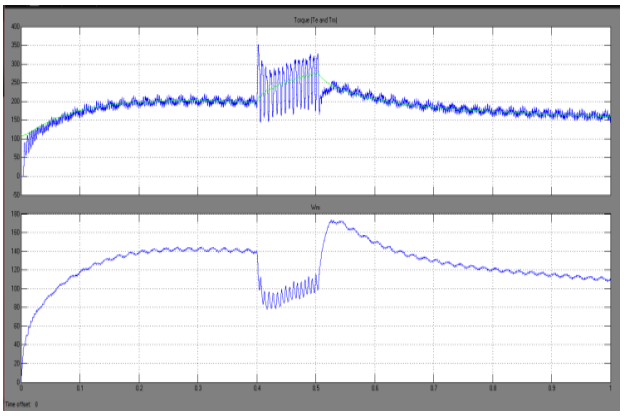

Fig:24 Torque (Tm and Te), Rotor speed

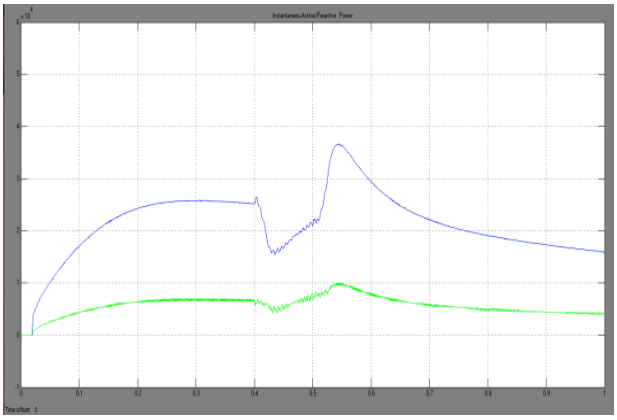

Fig. 25: Instantaneous Active and reactive power waveforms

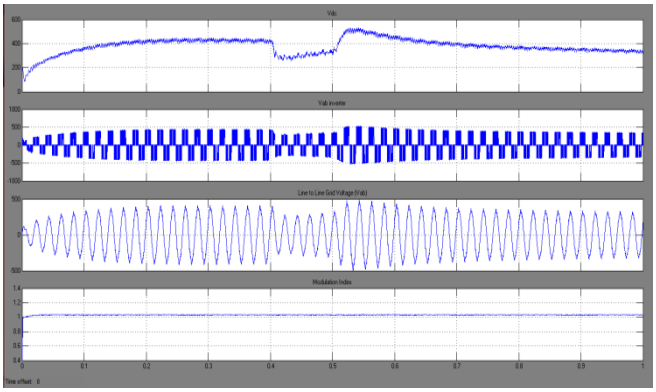

Fig. 26: Waveform of dc link voltage, Inverter output AC voltage, line to line grid voltage, and modulation Index.

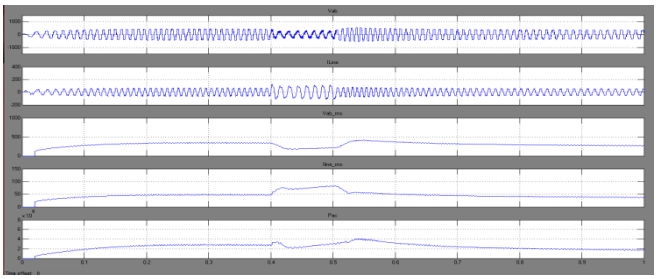

Fig. 27: Waveform of line to line Voltage (Vab), Line Current (IL), rms Line Voltage (Vab_rms), AC Power

## V. CONCLUSION

The dc-link capacitor provides decoupling between the generator-side and grid-side converter, a thereby offers separate control flexibilities for the power converters. The developed model and its control was simulated in MATLAB/SIMULINK and tested/validated for different conditions i.e. constant and variable wind speed, different faults like three phase to ground etc. The results presented showed good performances of the developed model and control. After the fault has cleared, various parameters regain their steady state values within short time, indicating the fastness of the control action.

## VI. REFERENCE


[1] Haque, M.E., Negnevitsky, M. and Muttaqi, K.M.,"A novel control strategy for a variable-speed wind turbine with a permanent-magnet synchronous generator," IEEE Transactions on Industry Applications, , vol. 46, no. 1, pp. 331-339, Jan/Feb. 2010.

[2] Zhang, S., Tseng, K.J., Vilathgamuwa, D.M., Nguyen, T.D. and Wang, X.Y. , " Design of a robust grid interface system for PMSG-based wind turbine generators," IEEE Transactions on Industrial Electronics, vol. 58, no. 1, pp. 316-328, Jan. 2011.

[3] Kumar, V., Joshi, R.R. and Bansal, R.C., "Optimal control of matrix converter based WECS for performance enhancement and efficiency optimization," IEEE Transaction of Energy Conversion, vol. 24, no. 1, pp. 264-273, March. 2009.

[4] Bhende, C.N., Mishra, S. and Malla, S.G., "Permanent magnet synchronous generator-based standalone wind energy supply system," IEEE Transactions on Sustainable Energy, vol. 2, no. 4, pp. 361-373, Oct.. 2011.

[5] Xia, Y., Ahmed, K.H. and Williams, B.W. " A New Maximum Power Point Tracking Technique for Permanent Magnet Synchronous Generator Based Wind Energy Conversion System," IEEE Transactions *on Power Electronics*, vol. 26, no. 12, pp. 3609-3620, Dec. 2011.

[6] Koutroulis, E. and Kalaitzakis, K. , " Design of a maximum power tracking system for wind-energy-conversion applications," *IEEE Transactions on Industrial Electronics*, vol. 53, no. 2, pp.486-494,April 2006.

[7] Kenneth E. Okedu, S. M. Muyeen,RioTaka hashi, and Junji Tamura, " Wind farms fault ride through using DFIG with new protection scheme," *IEEE trans. On Sustainable Energy*, vol. 3, no. 2, pp.242-254, April 2012.

[8] B. Chitti Babu ,and K.B.Mohanty , " Doubly-fed induction generator for variable speed wind energy conversion systems-modeling & simulation," *International Journal of Computer and Electrical Engineering*, vol. 2, no. 1,pp. 1793-8163, Feb. 2010.

[9] Haining Wang, Chem Nayar, Jianhui Su, and Ming Ding, " Control and interfacing of a grid-connected small-scale wind turbine generator," *IEEE Trans.On Energy Convers.*, vol. 26, no. 2, pp.428-434, June 2011.

[10] Mahmoud M. Amin, and Osama A. Mohammed, " Development of high-performance grid-connected wind energy conversion system for optimum utilization of variable speed wind turbines," *IEEE Trans. On Sustainable Energy*, vol. 2, no. 3, pp.235-, July 2011.

[11] Johann W. Kolar, Thomas Friedli, Jose Rodriguez, , and Patrick W. Wheeler, "Review of three-phase PWM AC-AC converter topologies," *IEEE Trans. On Industrial Electronics*, vol. 58, no. 11, pp.4988-5066, Nov. 2011.

[12] C sasi. and Mohan G., "Performance analysis of grid connected wind energy conversion system with a PMSG during fault conditions, "*International journal of engineering and advanced technology* ,vol.2, no.4, pp.356-361, April 2013.



**First Author** : Manpreet Kaur
**Qualification**: B-Tech
Pursuing M-Tech (Electrical Eng.)
BGIET SANGRUR



**Second Author** : Prince Jindal,
**Qualification:** ME
Pursuing PHD in field of non conventional energy resources

.